An Inchworm-Inspired Motion Strategy for Robotic Swarms

Kasra Eshaghi*[ψ], Zendai Kashino[ψ], Hyun Joong Yoon[ϕ], Goldie Nejat[ψ], Beno Benhabib[ψ]

ψ Department of Mechanical and Industrial Engineering, University of Toronto, 5 King's College Road, Toronto, ON, M5S 3G8, Canada.

Φ School of Mechanical and Automotive Engineering, Daegu Catholic University, Hayang, Gyeongsan, Gyeongbuk 712-702, Republic of Korea

E-mails: kasra.eshaghi@mail.utoronto.ca, zendkash@mie.utoronto.ca, yoon@cu.ac.kr, nejat@mie.utoronto.ca, benhabib@mie.utoronto.ca

(Accepted __, First published online: __)

SUMMARY

Effective motion planning and localization are necessary tasks for swarm robotic systems to maintain a desired formation while maneuvering. Herein, we present an inchworm-inspired strategy that addresses both these tasks concurrently by using anchor robots. The proposed strategy is novel as, by dynamically and optimally selecting the anchor robots, it allows the swarm to maximize its localization performance while also considering secondary objectives, such as the swarm's speed. A complementary novel method for swarm localization, that fuses inter-robot proximity measurements and motion commands, is also presented. Numerous simulated and physical experimental examples are included to illustrate our contributions.

KEYWORDS: Swarm Robotics; Motion Planning; Swarm Localization; Millirobots, Multi-Robot Systems.

1. Introduction

Research on swarm robotic systems (SRSs), typically, refers to the study of autonomous teams that act as a single entity to achieve objectives that are beyond the capabilities of their individual members.[1-7] Inspired by biological swarms, they are characterized by their high degree of inter-robot coordination and the large number of member robots, employing decentralized, semi-centralized, or centralized control architectures.[8-11] Correspondingly, such swarm systems, often, balance desirable properties associated with decentralized architectures (*e.g.*, scalability to larger teams and robustness to the loss of members) with the relative simplicity of centralized control. In academia, SRSs are, commonly, investigated using millimeter scale robots, *millirobots.*[12-14]

An essential element in utilizing SRSs is the planning and control of their motion, which is often termed as formation control.[15] This process primarily involves the planning and controlling the motion of the individual member robots, while the overall swarm travels along a specified trajectory. Swarm localization, (i.e., determining the position of all swarm members), in this context, is important, especially, as localization errors directly translate to errors in motion commands and ineffective formation control. Past research has dealt with these issues (i.e., motion planning and localization), mostly, separately – in contrast to our research discussed herein that deals with both issues concurrently.

Approaches to swarm-motion planning, commonly, assume that member robots move from an initial formation to a destination one without an overall 'swarm-shape' (geometry/ configuration) control along a trajectory. They, typically, employ a decoupled two-phased approach: (i) planning the trajectories of the robots individually, and (ii) incorporating a separate coordination mechanism to

* Corresponding author. Email: kasra.eshaghi@mail.utoronto.ca

ensure inter-robot collisions are avoided.[16-20] Methods that do consider maintaining a desired swarm formation, while following a trajectory, on the other hand, are, typically, categorized as behavioral,[21-24] leader-follower,[25-28] or virtual-structure methods.[15,29,30] However, these approaches are subjected to a variety of constraints on formation as well as trajectory following. Other approaches to swarm-motion planning have, for example, investigated methods for area coverage and monitoring,[31,32] and collision free paths in real time.[33]

Approaches to swarm localization, mainly, focus on estimating the relative distances between robots,[12-14,34,35] or estimating the changes to the swarm's formation by using sample statistics from the swarm.[36-39] Methods of estimating the positions and orientations (poses) of all robots in the swarm by fusing sensing data and motion commands,[40-45] and methods that propose the use of external infrastructure, such as stationary beacons[46-49] (*e.g.,* GPS, NorthStar) and computer vision systems[50-52] (*e.g.,* AprilTag, WhyCon, OptiTrack) have also been suggested in the literature. The latter ones tend to be more accurate, as the use of external infrastructure would yield the same level of uncertainty independent of travelled distance. However, often, external infrastructure may not be readily available to assist with localization (*e.g*., in disaster zones) or even possible to use (*e.g.,* unstructured indoor environments). External infrastructures may also require additional hardware to be installed on the swarm robots – a difficult task due to the size limitations of millirobots used in swarm robotics research[12-14].

The few hybrid approaches to swarm-motion planning that also consider localization, typically, advocate the use of anchor robots.[53-57] Anchors represent robots that remain stationary, while other mobile units move to their destination. Use of anchors may improve the localization accuracy of the swarm as they provide stationary references (i.e., landmarks) that can be detected by other robots. In the methods discussed in refs. [53-55], the robots implement a leap-frogging strategy, where the robots take turns moving toward their destinations. These approaches select intermediate goal positions for the robots that maximize localization accuracy,[53,54] or plan robot paths that minimize the accumulated uncertainty in localization.[55] However, commonly, these have been developed for smaller teams of three to four robots and their formulation may not be scalable to larger swarms.

A method for localizing larger swarms was proposed in ref. [56], where robots move to their destination one at a time and update their respective estimated pose after each movement. This update fuses inter-robot proximity measurements, the estimated location of anchor robots, and the (single) mobile robot's motion command through an Extended-Kalman-Filter (EKF). The method presented in ref. [57] is, similarly, scalable to larger swarms. In the method, the swarm is randomly divided into two equal-sized subgroups that take turns in acting as anchors. After a predetermined time, all robots stop to localize themselves by fusing measurements to selected nearby anchors and are provided the next set of motion commands. The subgroups, then, switch roles. This two-step motion strategy, however, requires the team to be divided into subgroups prior to deployment, thus, preventing the swarm from selecting anchors dynamically. This method also suggests that subgroups switch roles based on a pre-determined time interval (i.e., it requires robots to use a synchronized clock). Furthermore, it is assumed that all mobile robots can 'see' all anchors.

Herein, we propose an inchworm-inspired motion-planning strategy for swarm trajectory following that employs dynamic anchor selection. Beyond past methods that use anchors in stricter roles, our novel strategy allows (a) the balancing of swarm-motion speed versus accuracy per users' needs (*i.e.,* flexibility), and (b) the use of any localization method (*i.e.,* modularity).

In contrast to methods that limit the robots to moving one at a time or, for example, through two-grouped motion, our proposed strategy achieves flexibility by allowing the swarm to dynamically select the number and choice of robots that act as anchors. In addition to meeting a motion-speed versus accuracy requirement, adjusting the choice of anchors also allows the swarm to meet run-time practical constraints, such as the finite communication range between robots.

Abovementioned modularity is achieved by decoupling the two main problems at hand – i.e., determining (*i*) an effective swarm-motion planning strategy, and (*ii*) an accurate global swarm-localization method. It is conjectured that accurate swarm motion can only be achieved via accurate global localization. The work presented herein, also, marks one of the first swarm-motion planning strategies designed to work with any localization method.

A complementary novel localization method that efficiently and effectively fuses local swarm-formation estimates with motion information to localize the swarm in a global reference frame is also presented herein. In contrast to earlier approaches, this localization method does not require direct interactions between (all) the mobile and anchor robots. Namely, it can localize the swarm with partial information acquired from robots regarding their respective neighbors, as first discussed in our work reported in ref. [45].

2. Problem Definition

The objective of our study is to develop an effective motion-planning strategy for a swarm of n_r Robots, $\boldsymbol{R} = \{R_i\}_{i=1}^{n_r}$, as it travels along a desired trajectory, defined by a time-phased set of (swarm) configurations – a point-to-point (PTP) trajectory, Fig. 1 below.

In imitating an inchworm, the motion-planning sub-strategy to be developed would move the swarm between any two successive configurations (*i.e.*, points in PTP motion), Fig. 1, through multiple intermediate steps. In each intermediate step, some members of the swarm, designated as *anchor robots*, would remain stationary, while others, designated as *mobile robots*, would travel to the next desired configuration.

As discussed earlier in the Introduction, and illustrated in our investigations, a key variable in an inchworm-inspired sub-strategy is the selection of anchors for every incremental step – namely, the selection of both the number of anchors, n_a, as well as the choice of anchor robots, $\boldsymbol{R}_a$. It is conjectured that such selections would have a tangible impact on the performance of an inchworm motion, especially, for accurate trajectory tracking. A primary problem addressed in this paper is, thus, the optimal selection of anchors during runtime.

Effective swarm trajectory following, with high fidelity, is also conjectured to depend on accurate localization during runtime. However, one must note that, localization performance for swarms that utilize inchworm-type trajectory following would be directly affected by the speed requirement for the task at hand. Namely, the faster the speed of the swarm, the lower number of anchor robots that can be used by the inchworm motion sub-strategy, thus, resulting in reduced localization and motion accuracy. This presents us with a dilemma: one would like to have higher number of anchors for better motion accuracy, though this would come at a price of slower motion.

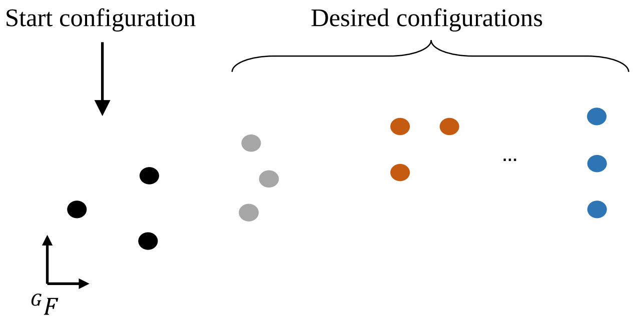

Fig. 1. PTP trajectory swarm motion.

The abovementioned two issues are closely interdependent and need to be treated concurrently. In this context, a measure of *swarm speed performance*, P_v, is first defined herein by:

$$P_v(n_a) = \frac{v(n_a)}{v_{max}}, \tag{1}$$

where $v(n_a),$ is a representation of the achievable speed of a swarm operating with n_a anchors, normalized with respect to a representation of the maximum speed achievable by the swarm with no anchors, v_{max}.

Similarly, a measure of *swarm localization performance*, P_l, is defined by:

$$P_l(n_a, \boldsymbol{R}_a) = \frac{e_l(n_a, \boldsymbol{R}_a)}{e_{l,max}}, \tag{2}$$

where $e_l(n_a, \boldsymbol{R}_a)$ is the localization error for a swarm operating with a specific selection of anchor robots, $(n_a, \boldsymbol{R}_a)$, normalized with respect to the worst-case localization error of the swarm with no anchors, $e_{l,max}$.

In this work, thus, we propose that, anchor selection for the proposed inchworm sub-strategy should aim to maximize an overall swarm motion performance metric, P_s, defined by:

Maximize:

$$P_s(n_a, \boldsymbol{R}_a) \ = w_v P_v(n_a) \ - w_l P_l(n_a, \boldsymbol{R}_a), \tag{3}$$

subject to:

$$\begin{aligned} g(n_a, \boldsymbol{R}_a) \ &\leq 0 \\ h(n_a, \boldsymbol{R}_a) \ &= 0' \end{aligned} \tag{4}$$

where w_v and w_l are weights denoting the importance of the swarm speed and localization performance, $(w_v + w_l = 1)$, and, $g(n_a, \boldsymbol{R}_a)$ and $h(n_a, \boldsymbol{R}_a)$ represent swarm motion constraints (*e.g.*, connectivity, speed, and desired configuration feasibility).

One can recall that Eq. (3) needs to be solved in an online manner. Furthermore, in addition, the swarm-localization process also needs to be formulated for runtime solution with potentially limited measurement data.

3. Overview of Proposed Swarm-Motion Strategy

As described above, the objective of our study is to develop an effective motion-planning strategy for a swarm to travel along a desired trajectory, defined by a time-phased set of (swarm) configurations – a point-to-point (PTP) trajectory, Fig. 1. In this context, the inchworm-inspired motion sub-strategy moves the swarm between two successive configurations, as part of the desired PTP trajectory, over multiple incremental steps. The inchworm sub-strategy (*a*) dynamically selects the optimal anchor robots for each successive move between two desired configurations in order to maximize the swarm's overall motion performance, detailed in Section 4 below, and (*b*) it also re-estimates the swarm configuration after every incremental move of the inchworm motion, detailed in Section 5 below. Continuous repetition of the inchworm-inspired motion sub-strategy allows the swarm to follow the desired PTP trajectory.

An overview of the proposed inchworm sub-strategy between two successive configurations, in the context of PTP swarm motion, is presented in Fig. 2 below. In this figure and onward, in this paper, any swarm configuration, C, is defined as the set of all global robot positions (in the swarm):

$$C \ = \{{}^G\boldsymbol{x}_i\}_{i=1}^{n_r}, \tag{5}$$

where ${}^G\boldsymbol{x}_i = ({}^Gx_i, {}^Gy_i)$ represents the position of Robot *i* with respect to the global reference frame, ${}^GF$.

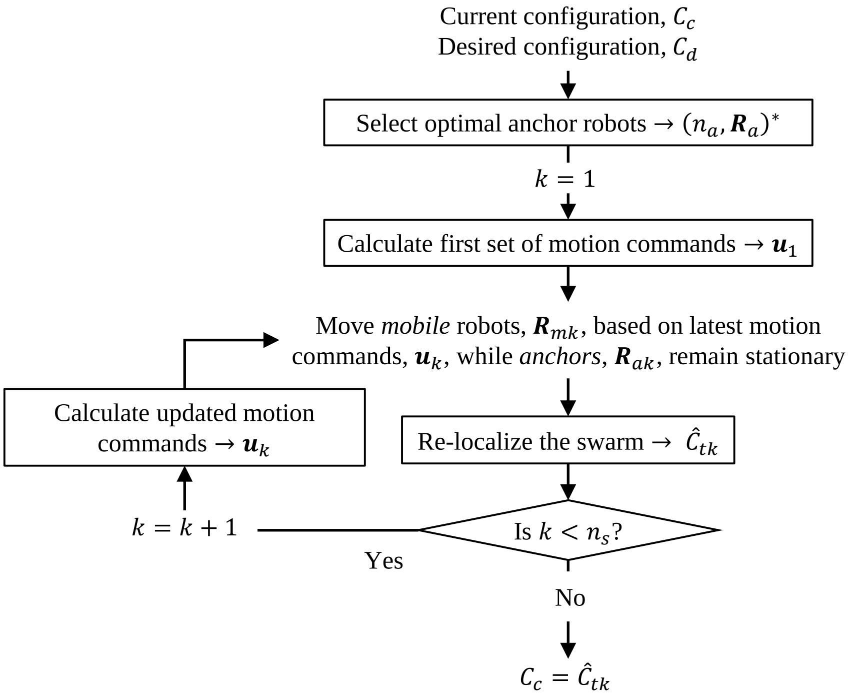
Current configuration, C_c
Desired configuration, C_d
Select optimal anchor robots → $(n_a, \boldsymbol{R}_a)^*$
$k = 1$
Calculate first set of motion commands → $\boldsymbol{u}_1$
Move *mobile* robots, $\boldsymbol{R}_{mk}$, based on latest motion commands, $\boldsymbol{u}_k$, while *anchors*, $\boldsymbol{R}_{ak}$, remain stationary
Calculate updated motion commands → $\boldsymbol{u}_k$
Re-localize the swarm → $\hat{C}_{tk}$
$k = k + 1$
Is $k < n_s$?
Yes
No
$C_c = \hat{C}_{tk}$

Fig. 2. The proposed swarm-motion strategy in the context of swarm-motion execution.

In Fig. 2 above, for a given ‘couple’ of successive configurations, *i.e.*, the swarm’s (first) current and (next) desired configurations, C_c and C_d, respectively, the proposed inchworm sub-strategy:

(*i*) Selects the optimal set of anchor robots, $(n_a, \boldsymbol{R}_a)^*$, to use in all the steps of the incremental (iterative) motion toward C_d, and, consequently, determines the necessary number of steps to move the swarm from C_c to C_d, n_s;

Sets iteration/step number $k = 1$;

(*ii*) Calculates the motion commands for the (first) set of mobile robots, based on C_c and C_d, $\boldsymbol{u}_1$;

(*iii*) Moves (only) the *mobile* robots, for the iteration at hand, $\boldsymbol{R}_{mk}$, to their destination on C_d, based on the latest motion commands, $\boldsymbol{u}_k$, while the anchors, $\boldsymbol{R}_{ak}$, remain stationary – it must be noted that C_d would only be achieved in approximation due to a multitude of errors (including robot motion errors);

(*iv*) Re-localizes the swarm, after the motion of all the mobile robots has been completed, and obtains an estimate of the latest (true) swarm configuration (filled dots in Fig. 3*(b)-(d)*), $\hat{C}_{tk}$;

If there are remaining mobile robots to move, i.e., $k < n_s$, sets iteration number $k = k + 1$ and continues to (*v*) below, otherwise, sets $C_c = \hat{C}_{tk}$ and exits the loop.

(*v*) Re-calculates the motion commands for the next set of mobile robots based on C_d and the latest $\hat{C}_{tk}$, and returns to (*iii*) above.

It can be noted that the optimal anchor selection step of the proposed swarm-motion strategy is completed in a centralized manner. The remaining components, which include the calculation and execution of motion commands, and the necessary steps for re-localization, however, can be completed in a decentralized manner to promote scalability and robustness.

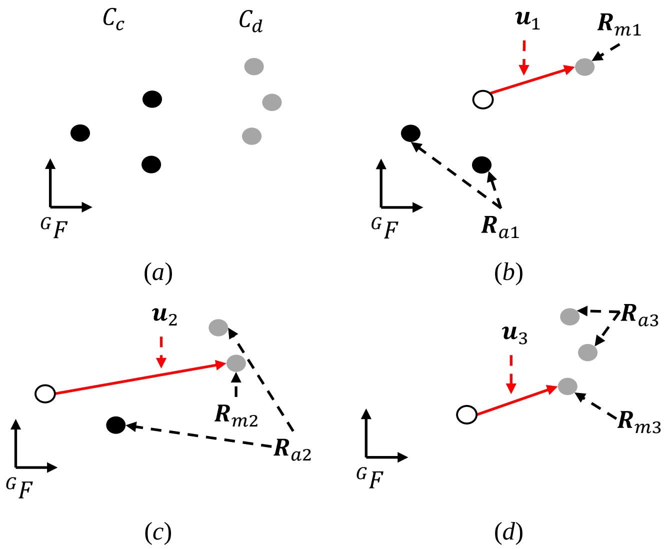

Fig. 3. The proposed inchworm-motion sub-strategy: (*a*) current and desired configurations, C_c, C_d, (*b*)-(*d*) intermediate estimated swarm configurations (filled circles), $\hat{C}_{tk}$ for steps $k = 1, 2, 3$, respectively.

The proposed inchworm sub-strategy is illustrated in Fig. 3 above, for a swarm of three robots, with one mobile robot at a time. The motion strategy is novel in that it allows the swarm to dynamically select the (number and choice of) anchor robots as it travels through a sequence of configurations. This (*flexibility*) feature is used herein to maximize the motion performance (speed and localization) of the swarm, Eq. (3). One can note that dynamic anchor selection could also facilitate the consideration of other objectives, including, for example, maintenance of a desired degree of connectivity in the swarm. Additionally, repeatedly estimating the intermediate configurations of the swarm allows us to enhance the estimated position of anchor robots and, as a result, provide more accurate motion commands.

4. Proposed Inchworm-Motion Sub-Strategy

The inchworm-motion sub-strategy outlined above requires the dynamic selection of optimal anchor robots for every step of (multi-step) motion between two successive swarm configurations. Herein, we present a novel search method which determines $(n_a, \boldsymbol{R}_a)^*$ that maximize the swarm's motion performance, Eq. (3), as it moves from C_c to C_d.

4.1. Optimization metrics for anchor selection

In Eq. (1), for the proposed inchworm-motion sub-strategy, the swarm's speed can be represented as the inverse of the number of steps required to reach to desired configuration, n_s:

$$v(n_a) = \frac{1}{n_s(n_a)}, \qquad (6)$$

where

$$n_s(n_a) = \frac{n_r}{n_r - n_a}. \qquad (7)$$

As per Eq. (6), the maximum achievable swarm speed corresponds to a swarm operating with zero anchors (*i.e.*, $n_a = 0, v_{max} = v(0) = 1$). It should also be noted that only anchor numbers that result in an integer number of incremental motion steps, n_s, are considered *feasible*. For example, for a swarm of $n_r = 10$ robots, the feasible number of anchors would be $n_a = 0, 5, 8,$ or 9.

The localization error of the swarm for a given choice of anchors, in turn, can be defined as the mean distance between the true and estimated positions of all robots once all robots have reached C_d (*i.e.*, all n_s steps are completed):

$$e_l(n_a,\boldsymbol{R}_a) \ = \frac{1}{n}\sum_{i=1}^{n_r}\left|{}^G\boldsymbol{x}_{tn_si} - {}^G\widehat{\boldsymbol{x}}_{tn_si}\right|, \tag{8}$$

where ${}^G\boldsymbol{x}_{tn_si}$ and ${}^G\widehat{\boldsymbol{x}}_{tn_si}$ are the true and estimated positions of Robot *i* in Configurations C_{tn_s} and $\hat{C}_{tn_s}$, respectively. It is important to clarify that, in our simulations, C_{tn_s} is calculated based on the noisy motion of the individual robots, whereas $\hat{C}_{tn_s}$ is an estimate of this (localized) swarm configuration, after the last step, using the proximity sensors on the individual robots.

A thorough investigation into anchor selection, which included extensive simulated experiments, verified that the number and choice of anchors have a meaningful impact on swarm-motion speed and post-movement localization accuracy, Eq. (6) and Eq. (8), respectively. These investigations have also indicated that the worst-case localization error would correspond to a swarm operating with no anchors (*i.e.*, $n_a = 0$, $e_{l,max} = e_l(0,\emptyset)$). The results of these investigations are summarized below.

4.1.1. Effect of the Number of Anchors. In this paper, it is conjectured that the number of anchors affects both the speed and localization performance of the swarm. With a greater number of anchors, fewer *mobile* robots can move at any one time and the swarm must go through more steps to reach the desired configuration. As noted above, the swarm's speed can be represented as the inverse of the number of steps required to completely move the swarm to a desired configuration, Eq. (6). This representation suggests that the swarm's speed and, thus, its corresponding performance, P_v, decreases linearly with increased number of anchors. Furthermore, the maximum achievable speed of the swarm corresponds to one's operating with no anchors.

Regarding swarm localization performance, extensive series of simulations were conducted. In these, a swarm of n_r robots was instructed to move from one (same) starting configuration, C_c, to another (random) desired configuration, C_d, using the proposed inchworm motion strategy. For each incremental motion step, a fixed number of n_a robots were designated as anchors while the other robots moved directly and concurrently to their next destination. Once the inchworm motion was completed, noisy sensor measurements were simulated and used to estimate the swarm's configuration. For each motion simulation experiment, a swarm localization error, $e_l(n_a,\boldsymbol{R}_a)$ was, then, calculated through Eq. (8).

1,000 random experiments were simulated for a swarm size of $n_r = 10$ robots. Fig. 4(*a*)-(*d*) below show the localization error obtained for cases with (*a*) zero, (*b*) five, (*c*) eight, and (*d*) nine anchors, respectively. All simulations were subjected to different levels of noise in their inter-robot sensing and motion-command executions. The results are plotted as localization error *versus* average distance traveled by the robots in the swarm.

The simulation results indicate that an increase in the number of anchors reduces localization error, though, sub-linearly (*i.e.*, there are diminishing returns to designating more robots as anchors). The results also show that the worst-case localization error corresponds to the swarm that is operating without the use of anchor robots (*i.e.*, $e_{l,max} = e_l(0,\emptyset)$)

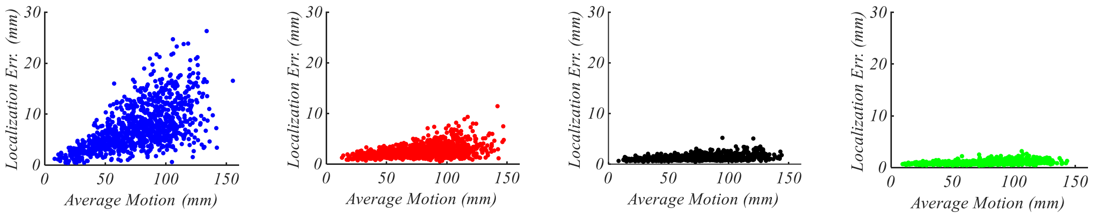

(*a*) (*b*) (*c*) (*d*)

Fig. 4. Swarm localization errors for (*a*) zero, (*b*) five, (*c*) eight, and (*d*) nine anchors, respectively.

4.1.2. Effect of the Choice of Anchors. It is further conjectured, herein, that the specific choice of anchors does not have a tangible impact on the speed of the swarm, though, it could affect localization. A series of simulated experiments was, thus, conducted to validate the conjecture that the choice of anchors indeed has an impact on swarm-localization performance. In this set of experiments, random desired configurations were generated. Then, for each random desired configuration, corresponding swarm inchworm motion was simulated for all possible combinatoric choices of anchors for a fixed n_a. The results of simulated motion and the subsequent estimations were evaluated in terms of the localization error, $e_l(n_a, \boldsymbol{R}_a)$, Eq. (8).

1,000 random experiments were simulated for a swarm size of $n_r = 10$ robots, where $n_a = 5$ robots remain stationary at a time. For such a case, there exist a total of 252 possible 5-robot anchor selections. All simulations were initialized with the same uncertain estimate of the swarm's initial configuration, C_c. All simulations were also subjected to different levels of noise in their inter-robot sensing and motion command executions.

Fig. 5(*a*)-(*d*) below show the localization errors for the (*a*) no anchors, (*b*) random anchors, (*c*) global worst anchors, and (*d*) global best anchors cases, respectively. The results are plotted as localization error *versus* average distance traveled by the robots in the swarm. A global worst/best represent the results of the choice of anchors that achieved the highest/lowest localization error for a given desired configuration, respectively. Moreover, random anchors represent the localization error associated with a choice of anchors that was selected randomly from the 252 possible choices. The results indicate that, for a given set of possible anchors, there exists an optimal sub-set to choose from that would result in the minimum possible localization error, $\boldsymbol{R}_a^*(n_a)$.

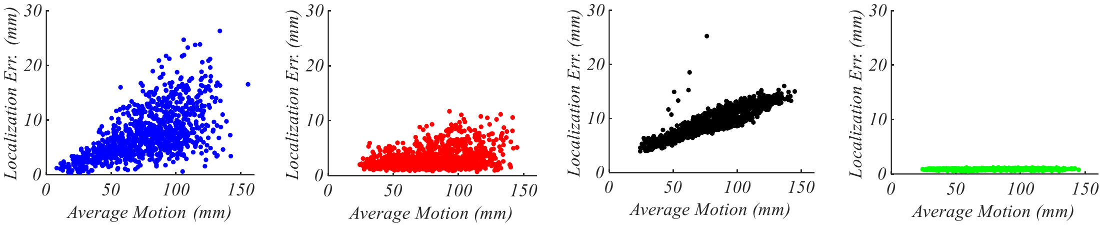

(*a*) (*b*) (*c*) (*d*)

Fig. 5. Swarm localization errors for different combinations of anchors: (*a*) zero anchors, (*b*) random anchors, (*c*) global worst anchors, and (*d*) global best anchors.

4.2. Search algorithm

The proposed search algorithm for $(n_a, \boldsymbol{R}_a)^*$ comprises two nested loops, Fig. 6 below. Assuming knowledge of the swarm's initial (pre-motion) configuration, C_c, the search begins by, first, determining v_{max} and $e_{l,max}$. Then, the outer optimization loop (Fig. 6, *red dashed line*) seeks the optimal number and choice of anchors by searching through the space of all feasible number of anchor robots. The inner loop (Fig. 6, *blue dashed line*), in turn, determines the best choices of anchors for n_a considered by the outer loop.

4.2.1. Outer optimization loop. Determination of the optimal number of anchors, n_a^* could be conducted by searching through the space of all feasible numbers using a simple (single, discrete-variable) search engine. For a (feasible) number of anchors considered in this outer loop, the corresponding optimal choices of anchors, $\boldsymbol{R}_a^*(n_a)$, would, then, be determined through the inner optimization loop described below.

One must note that the expected localization error of the swarm with any number of anchors at hand, $e_l\left(n_a, \boldsymbol{R}_a^*(n_a)\right)$, would also be returned from the inner loop. This measure would, then, be used in Eq. (3) to calculate the swarm's overall motion performance for the number of anchors considered in this outer loop, to eventually determine the final set of optimal anchors, $(n_a, \boldsymbol{R}_a)^*$.

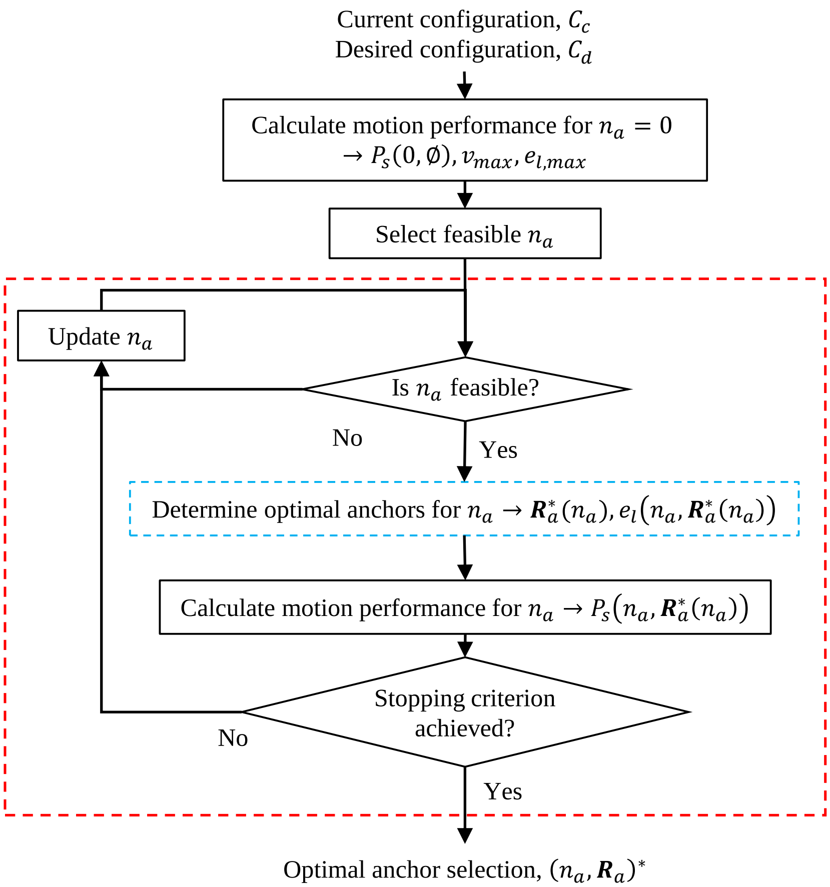
Current configuration, C_c
Desired configuration, C_d
Calculate motion performance for $n_a = 0$ → $P_s(0, \emptyset), v_{max}, e_{l,max}$
Select feasible n_a
Update n_a
Is n_a feasible?
No
Yes
Determine optimal anchors for n_a → $\boldsymbol{R}_a^*(n_a), e_l\left(n_a, \boldsymbol{R}_a^*(n_a)\right)$
Calculate motion performance for n_a → $P_s\left(n_a, \boldsymbol{R}_a^*(n_a)\right)$
Stopping criterion achieved?
No
Yes
Optimal anchor selection, $(n_a, \boldsymbol{R}_a)^*$

Fig. 6. The proposed optimal anchor robot selection method.

4.2.2. Inner optimization loop. For every feasible number of anchors considered, n_a, a search is carried out to determine the corresponding choice of anchors that yield minimum localization error. Namely, the inner optimization loop solves for:

$$\boldsymbol{R}_a^*(n_a) = \underset{\boldsymbol{R}_a(n_a)}{\arg\min}\, e_l\left(n_a, \boldsymbol{R}_a(n_a)\right). \tag{9}$$

Calculating the expected localization error for a given number and choice of anchors, $e_l\left(n_a, \boldsymbol{R}_a(n_a)\right)$, consists of simulating the inchworm motion, and computing the localization error once all robots execute their movement commands. All steps of the simulated inchworm motion, which include intermediate localization, are perturbed with noisy motion and proximity measurements to represent a realistic scenario.

One must note that the optimization problem at hand, Eq. (9), is an NP-hard combinatoric optimization problem with possible solutions numbering:

$$n_{sol} = \prod_{k=0}^{n_{steps}-1} \binom{n - kn_m}{n_m}, \tag{10}$$

where n_m is the number of mobile robots for each step of motion ($n_m = n_r - n_a$). It is, thus, recommended to use a combinatoric optimization method, such as a variation of the genetic algorithm, to guide which anchor choices to evaluate in this inner optimization loop. Furthermore, it is recommended to seed the search engine with high-quality initial solutions to expedite the optimization. A heuristic to produce one such high-quality initial solution, developed through our work, is proposed below.

4.2.3. Proposed Heuristic for Initial-Guess Selection. An initial guess of anchor robots can be chosen based on a variety of heuristics. Herein, we conjecture that the optimal choice of anchors for each incremental step towards the desired configuration is dependent on the underlying characteristics of the swarm's post-motion configuration.

In this regard, we propose two measures that encapsulate such characteristics: the expected *distribution* of the anchor robots, and the expected *separation* between the anchor and mobile robots. Namely, it is expected that the choice of anchors that maximize *distribution* and minimize *separation* in the post-motion configuration would result in relatively high localization accuracy. This heuristic was developed based on the proposed localization method used for the simulations in Section 4.1. Analysis of this method, detailed in Section 5 below, indicates that maximizing distribution and minimizing separation could maximize the influence of anchor robots and allow the swarm to achieve reduced localization errors.

A swarm's distribution is a measure of the area covered by the anchor robots. The swarm distribution, d_k, after *k* steps of the inchworm sub-strategy, can be defined as the average distance from the centroid of all anchor robots to all the individual anchors:

$$d_k(\boldsymbol{R}_{ak}) = \frac{1}{n_a}\sum_{i\in\boldsymbol{R}_{ak}}\left(\left|{}^{G}\hat{\boldsymbol{x}}_{tki} - {}^{G}\bar{\hat{\boldsymbol{x}}}_{tk\boldsymbol{R}_{ak}}\right|\right), \tag{11}$$

where $\boldsymbol{R}_{ak}$ are all anchor robots for the *k*th step, and ${}^{G}\bar{\hat{\boldsymbol{x}}}_{tk\boldsymbol{R}_{ak}}$ is the estimated centroid of these anchors.

A swarm's separation, conversely, is used to capture the connectivity between anchor and mobile robots. Separation, s_k, after *k* steps of the inchworm sub-strategy, can be defined as the difference between the centroid of the cluster of anchor robots and the centroid of the cluster of mobile robots:

$$s_k(\boldsymbol{R}_{ak}) = \left|{}^{G}\bar{\hat{\boldsymbol{x}}}_{tk\boldsymbol{R}_{ak}} - {}^{G}\bar{\hat{\boldsymbol{x}}}_{tk\boldsymbol{R}_{mk}}\right|, \tag{12}$$

where, ${}^{G}\bar{\hat{\boldsymbol{x}}}_{tk\boldsymbol{R}_{mk}}$ is the centroid of the mobile robots used in the *k*th step of the inchworm sub-strategy. For this initial heuristic, the position of mobile robots is calculated based on their provided motion commands.

The heuristic proposed for determining a high-quality initial solution for each step is, thus:

Maximize:

$$p_{ak}(\boldsymbol{R}_{ak}) = d_k(\boldsymbol{R}_{ak}) + \frac{1}{s_k(\boldsymbol{R}_{ak})}. \tag{13}$$

Results of extensive series of simulations in our work, as will be detailed in Appendix A, illustrated that anchors determined through the proposed heuristic would outperform random choices that can be used as an initial guess.

5. Proposed Swarm-Localization Method

The proposed inchworm motion sub-strategy requires the swarm's configuration to be re-estimated after each incremental step, Section 3. Herein, we present a novel localization method that obtains an estimate of the swarm's configuration, $\hat{C}_t$, by fusing an estimate of the swarm's (***true***) configuration, obtained based on motion commands, $\boldsymbol{u}_k$, $\hat{C}_{tu}$, with an estimate of the swarm's topology, obtained based on inter-robot ***proximity*** measurements, $\hat{T}_{tp}$. For simplicity, the index k is omitted in the following description of the localization method.

A swarm topology, as noted above, defines the positions of all the robots with respect to a local swarm frame, ${}^{L}F$, Fig. 7 below:

$$T = \{{}^{L}\boldsymbol{x}_i\}_{i=1}^{n_r}. \tag{14}$$

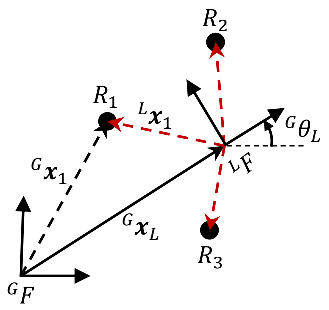

Fig. 7. Swarm topology.

As shown in Fig. 7 above, the swarm's topology can be related to its configuration through the pose of the local swarm frame with respect to the global frame, ${}^{G}F$, $({}^{G}\boldsymbol{x}_L, {}^{G}\theta_L)$. Namely, the position of Robot *i* with respect to ${}^{L}F$ can be transformed to ${}^{G}F$ through:

$${}^{G}\boldsymbol{x}_i({}^{L}\boldsymbol{x}_i, {}^{G}\boldsymbol{x}_L, {}^{G}\theta_L) = {}^{G}\boldsymbol{x}_L + {}^{G}R_L({}^{G}\theta_L){}^{L}\boldsymbol{x}_i, \tag{15}$$

where ${}^{G}R_L({}^{G}\theta_L)$ is the rotation matrix corresponding to the orientation of ${}^{L}F$ with respect to ${}^{G}F$:

$${}^{G}R_L({}^{G}\theta_L) = \begin{bmatrix} \cos({}^{G}\theta_L) & -\sin({}^{G}\theta_L) \\ \sin({}^{G}\theta_L) & \cos({}^{G}\theta_L) \end{bmatrix}. \tag{16}$$

Fig. 8 below presents an overview of the proposed two-phase localization method. Estimates of the swarm's configuration and topology are acquired in Phase 1 and subsequently fused in Phase 2.

The proposed localization method detailed below is novel in that it does not require direct interactions between all mobile and anchor robots. As long as the post-motion swarm configuration remains connected (*i.e.*, each robot can be sensed by at least one neighbor), the described method is applicable. This feature simplifies swarm trajectory planning and control, as the required degree of swarm-connectivity constraint is lower than would be for other localization methods. It must also be noted that, although the proposed localization method was developed, primarily, for our inchworm swarm-motion strategy, it would, certainly, be usable by all robotic swarms equipped with the necessary sensing technology.

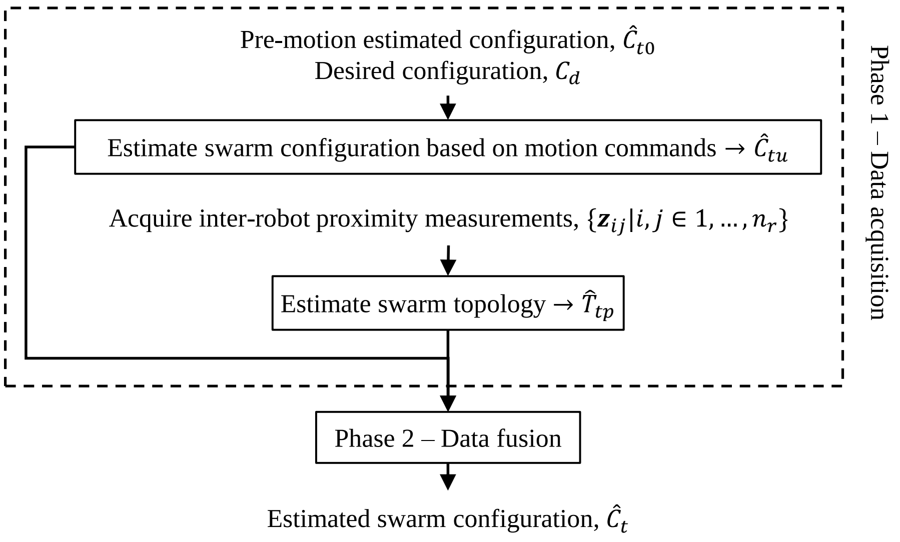
Pre-motion estimated configuration, $\hat{C}_{t0}$
Desired configuration, C_d
Estimate swarm configuration based on motion commands → $\hat{C}_{tu}$
Acquire inter-robot proximity measurements, $\{\boldsymbol{z}_{ij} | i, j \in 1, \dots, n_r\}$
Estimate swarm topology → $\hat{T}_{tp}$
Phase 1 – Data acquisition
Phase 2 – Data fusion
Estimated swarm configuration, $\hat{C}_t$

Fig. 8. The proposed swarm-localization method.

5.1. Phase 1 – Data acquisition

In Phase 1, (1) a preliminary configuration estimate, in the global (motion) frame, ${}^{G}F$, and (2) a topology estimate, in the local (swarm) frame, ${}^{L}F$, are obtained independently.

5.1.1. Phase 1.1: Preliminary swarm-configuration estimation. A preliminary estimate of the swarm's configuration, after an incremental step of the inchworm sub-strategy, can be determined by assuming the motion commands of the mobile robots were executed with no uncertainty. A vector representing the change in position of Robot i, $\hat{\boldsymbol{u}}_i$, is used in our formulation. Since it is assumed that no odometry is available, this vector represents the difference between Robot i's desired position, ${}^{G}\boldsymbol{x}_{di}$, and pre-motion estimated position, ${}^{G}\hat{\boldsymbol{x}}_{t0i}$, respectively. For the mobile robots $\boldsymbol{R}_m$:

$$\hat{\boldsymbol{u}}_i = {}^{G}\boldsymbol{x}_{di} - {}^{G}\hat{\boldsymbol{x}}_{t0i}, i \in \boldsymbol{R}_m, \tag{17}$$

whereas, for anchor robots, $\boldsymbol{R}_a$:

$$\hat{\boldsymbol{u}}_i = 0, i \in \boldsymbol{R}_a, \tag{18}$$

A preliminary estimate of the post-motion configuration of the swarm, $\hat{C}_{tu} = \left\{{}^{G}\hat{\boldsymbol{x}}_{tui}\right\}_{i=1}^{n_r}$, can, then, be acquired by applying the above defined motion commands:

$${}^{G}\hat{\boldsymbol{x}}_{tui} = {}^{G}\hat{\boldsymbol{x}}_{t0i} + \hat{\boldsymbol{u}}_i, i \in \{1, \dots, n\}. \tag{19}$$

Fig. 9 below presents a preliminary configuration estimate acquired for the first step of the inchworm sub-strategy in Fig. 3, after the motion of R_1.

Due to the uncertainty in motion command execution, the swarm configuration estimated via Eq. (19) would have uncertainty associated with it, denoted as $\Delta_u = \{\, \delta_{ui}\}_{i=1}^{n_r}$, where δ_{ui} is the uncertainty in the estimated position of Robot i. This uncertainty is dependent on the motion model of individual robots.

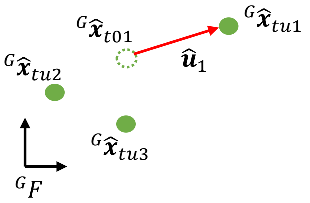
${}^{G}\hat{\boldsymbol{x}}_{t01}$
${}^{G}\hat{\boldsymbol{x}}_{tu1}$
$\hat{\boldsymbol{u}}_1$
${}^{G}\hat{\boldsymbol{x}}_{tu2}$
${}^{G}\hat{\boldsymbol{x}}_{tu3}$
${}^{G}F$

Fig. 9. A preliminary swarm-configuration estimate.

5.1.2. Phase 1.2: Swarm-topology estimation. The post-motion topology of the swarm, $\hat{T}_{tp} = \left\{{}^{L}\hat{\boldsymbol{x}}_{tpi}\right\}_{i=1}^{n_r}$, can be estimated by fusing inter-robot proximity measurements acquired by all the robots. These measurements comprise distance and bearing information describing the relative locations of neighboring robots. Namely, Robot i's observation of Robot j, can be described by:

$$\boldsymbol{z}_{ij} = \left(\rho_{ij}, \varphi_{ij}\right). \tag{20}$$

where ρ_{ij} and φ_{ij} are, respectively, the distance and bearing of Robot j, with respect to Robot i, as observed by Robot i.

Herein, it is proposed to fuse the inter-robot proximity measurements using a modified version of a swarm-topology estimation approach previously developed in our lab at the University of Toronto.[45] In this approach, data fusion is achieved by clustering all observations of individual robots and calculating respective centroid positions. The primary modification made herein is a reformulation of the clustering objective function, as will be detailed in Appendix B.

It should be noted that, in addition to a swarm topology estimate, $\hat{T}_{tp}$, the proposed method also provides a measure of topology-estimation uncertainty, $\Delta_p = \{\, \delta_{pi}\}_{i=1}^{n_r}$, where δ_{pi} is the uncertainty in the estimated position of Robot i.

An example estimated topology, with respect to ${}^{L}F$, that was acquired using sensing data gathered after R_1 has completed its move (Fig. 3(b)) is shown in Fig. 10 below.

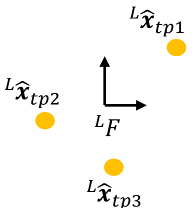
${}^{L}\hat{\boldsymbol{x}}_{tp1}$
${}^{L}\hat{\boldsymbol{x}}_{tp2}$
${}^{L}F$
${}^{L}\hat{\boldsymbol{x}}_{tp3}$

Fig. 10. A post-motion swarm-topology estimate.

5.2. Phase 2 – Data fusion

Phase 2 of the proposed swarm-localization method estimates the post-motion swarm configuration by superimposing $\hat{C}_{tu}$ and $\hat{T}_{tp}$. Namely, the proposed method seeks to determine the pose for ${}^{L}F$ defined with respect to ${}^{G}F$ that minimizes the distances between corresponding robot positions in the post-motion swarm configuration and topology estimates:

$$\left({}^{G}\boldsymbol{x}_{L}^{*}, {}^{G}\theta_{L}^{*}\right) = \underset{\left({}^{G}\boldsymbol{x}_{L}, {}^{G}\theta_{L}\right)}{\arg\min} \sum_{i=1}^{n_r} w_i \left| {}^{G}\hat{\boldsymbol{x}}_{tpi}\left({}^{L}\hat{\boldsymbol{x}}_{tpi}, {}^{G}\boldsymbol{x}_{L}, {}^{G}\theta_{L}\right) - {}^{G}\hat{\boldsymbol{x}}_{tui} \right|^2, \tag{21}$$

where ${}^{G}\hat{\boldsymbol{x}}_{tpi}\left({}^{L}\hat{\boldsymbol{x}}_{tpi}, {}^{G}\boldsymbol{x}_{L}, {}^{G}\theta_{L}\right)$ is the position of Robot *i* based on inter-robot proximity measurements, transformed to ${}^{G}F$ through Eq. (15)

The weights of the superimposition step are selected to reflect the uncertainty in the estimated positions in the preliminary estimates from Phase 1. Specifically, the weights are considered to be inversely proportional to (*a*) the uncertainty in robot positions in the swarm-topology estimate, δ_{pi}, and (*b*) the uncertainty in the motion command execution of the same robot, δ_{ui}. The weight associated with Robot *i* is, thus, defined as:

$$w_i = \frac{1}{\delta_{pi} + \delta_{ui}}. \tag{22}$$

This scheme, typically, results in the positions of anchor robots being weighted higher than the positions of mobile robots. This is due to their lack of motion and higher positional certainty in the preliminary configuration estimate.

Upon completion of the superimposition step, a robot's updated position can be calculated as its mean position in the superimposed configuration and topology:

$${}^{G}\hat{\boldsymbol{x}}_{ti} = \frac{{}^{G}\hat{\boldsymbol{x}}_{tpi}\left({}^{L}\hat{\boldsymbol{x}}_{tpi}, {}^{G}\boldsymbol{x}_{L}^{*}, {}^{G}\theta_{L}^{*}\right) + {}^{G}\hat{\boldsymbol{x}}_{tui}}{2}, i \in 1, \ldots, n_r. \tag{23}$$

The set of all final estimated positions form the final swarm configuration estimate, $\hat{C}_t$

An example showing the superimposition of the swarm topology estimate, Fig. 10, onto the swarm configuration estimate after the first step of inchworm motion in Fig. 9, is shown in Fig. 11 below. It can be noted that robots which are further from the center of the swarm's topology have a higher influence on the superimposition step and, in turn, on the estimated position of the swarm's topology. Namely, small changes in their position results in a significant increase of the objective function in Eq. (21), when compared to small changes in the position of robots that are close to the swarm's center. This feature is used, herein, to select the heuristic for the choice of anchors, Section 4. The proposed heuristic effectively selects robots that are far from the swarm's center (*i.e.,* maximize distribution) as anchors, and robots that are close to the swarm's center (*i.e.,* minimize separation) as mobile robots. As a result, anchors that have a higher position certainty have a larger influence on the estimated position of the swarm topology and, thus, reduce the localization errors of the swarm.

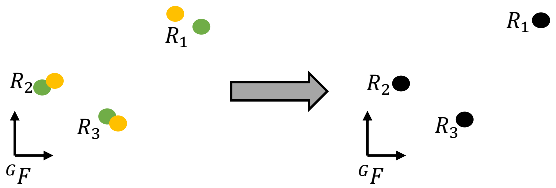

Fig. 11. Updated post-motion swarm configuration.

5.3. Comparison to Graph SLAM

One may note similarities between the proposed localization method and Graph SLAM[58] – a common method for addressing the single robot simultaneous localization and mapping (SLAM) problem. Namely, if applied to swarm localization, Graph SLAM could equate anchors to stationary landmarks and estimate the swarm's configuration by clustering the inter-robot sensor measurements while simultaneously superimposing them onto the executed motion commands. This would differ from the sequential approach proposed in this paper in that, in Graph SLAM method, inter-robot sensor measurements and motion commands are considered simultaneously. Namely, in our method, inter-robot sensor measurements are clustered in Phase 1.2 (Swarm-topology estimation) and superimposed onto motion commands in Phase 2 (Data fusion).

There are two main advantages to the sequential nature of the proposed localization method: (*i*) design modularity, and (*ii*) consideration of millirobot limitations. The design modularity of the proposed localization method is achieved as the inter-robot sensor measurements and motion commands are considered in two independent steps. This simplifies future improvements and allows for the parallel development of pertinent solutions – for example, different clustering functions for topology estimation, or different approaches to estimating the position of the swarm's topology may be considered. The sequential nature of the proposed localization method also considers the communication and computational limitations of millirobots used in swarm robotic research. Namely, considering inter-robot sensor measurements and motion commands separately allows for reducing the amount of information that would need to be shared, within a swarm network, and processed by a central (*e.g.*, leader) robot. This reduces the risk of saturating the communication channels, memory, and processing power of millirobots, and yields in a more feasible localization method.

6. Illustrative Examples

Herein, we present multiple simulated and physical experiments illustrating the proposed PTP inchworm-inspired swarm motion strategy.

6.1. Swarm Motion Simulations

6.1.1. A detailed trajectory-following example. The example considered herein aims to illustrate the details of the proposed inchworm sub-strategy in following the desired PTP trajectory in Fig. 12 below. During the inchworm motion, the optimal number and choice of anchor robots are selected using the method detailed in Section 4, with performance weights chosen as $w_v = 0.5$, and $w_l = 0.5$. All motion commands, comprising straight-line paths, were subjected to zero-mean normally-distributed noise. Similarly, inter-robot proximity measurements, were also subjected to zero-mean normally-distributed noise.

Detailed results for motion of the simulation are illustrated in Fig. 13 below, where the hollow circles represent the locations of robots in all past (*red*/desired, *green*/estimated, and *blue*/true) swarm configurations, while the solid circles represent the locations of robots in all next (desired, estimated, and true) configurations in each step of motion. In this example, the optimal anchor selection method chose $n_a = 5$ anchors to achieve all three desired configurations: for C_{d1}, the optimal anchor robots for the first step of the two-step motion were $\boldsymbol{R}_{a1} = \{R_2, R_4, R_6, R_9, R_{10}\}$.

6.1.2. Another trajectory-following example. The proposed inchworm sub-strategy is further demonstrated herein for an example trajectory comprising 50 desired configurations, Fig. 14 below.

As one can note, the proposed strategy achieves high trajectory-following fidelity, in the global motion frame, over a substantial distance travelled, without any feedback.

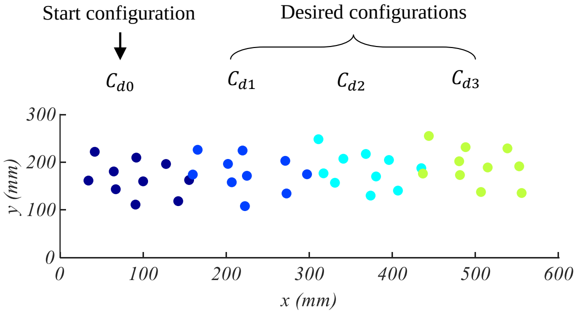

Fig. 12. An example PTP trajectory.

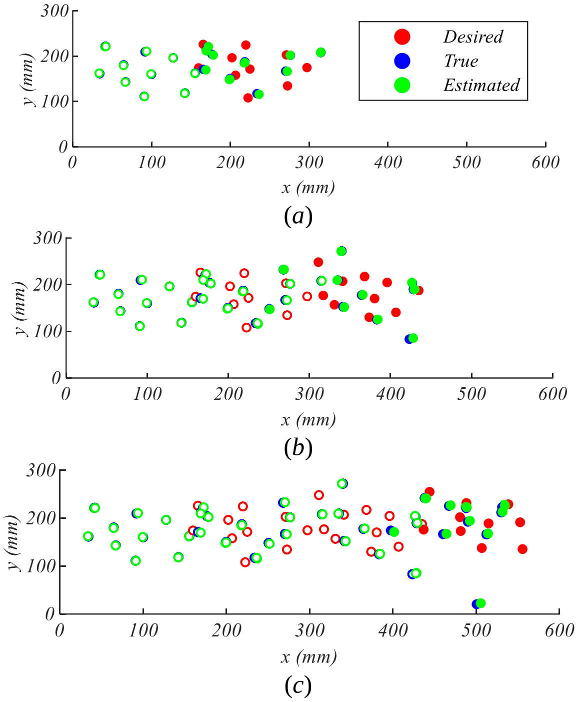

Fig. 13. PTP swarm trajectory – Example 1: swarm configurations after achieving the (*a*) first, (*b*) second, and (*c*) third configuration, respectively.

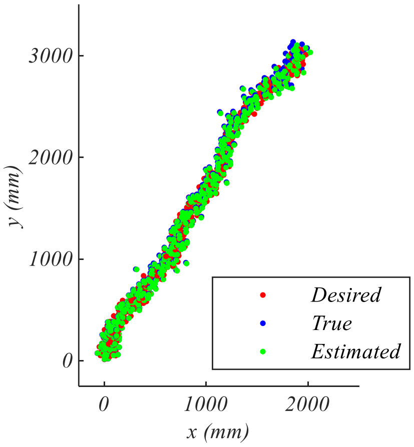

Fig. 14. PTP swarm trajectory – Example 2.

6.2. Swarm Motion Experiments

In the experiments detailed herein, a swarm of millirobots (*mROBerTOs*) is instructed to follow a desired (swarm) trajectory – defined by a set of time-phased distinct configurations. Members of the swarm individually translate and rotate along the given trajectory to achieve the desired configurations, successively.

mROBerTO 2.0, developed in our lab at the University of Toronto,[12-14] is a millimeter-scale robot with a swarm sensing module that allows it to accurately measure the relative proximity of nearby robots through IR communication, Fig. 15 below.

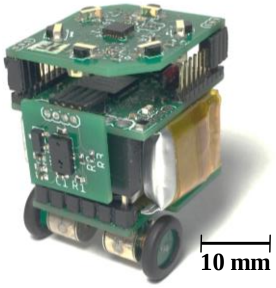

Fig. 15. *mROBerTO* 2.0.

For swarm localization, inter-robot proximity measurements, obtained by all robots individually in a decentralized manner, are sent to a host computer through ANT communication. Here, they are used to estimate the configuration of the swarm through the process detailed in Section 5. The central computer is also used to select the optimal anchors through the process detailed in Section 4, and to provide updated motion commands for the mobile robots in each step of the inchworm motion. The provided motion commands are executed by the robots in an open-loop and decentralized manner without any intervention from the host computer.

The specific experiments discussed herein were conducted with a swarm of $n_r = 6$ *mROBerTO*s that were instructed to follow a trajectory with $n_d = 9$ desired configurations. With performance weights chosen as $w_v = 0.5$, and $w_l = 0.5$, the swarm used $n_a = 3$ anchors to move between all successive configurations.

Fig. 16 below illustrates the swarm's final desired (*red*), true (*blue*), and estimated (*green*) configurations, once the trajectory is completed. Fig. 17(*a*)-(*b*) below are the corresponding plots of the swarm localization and trajectory following errors versus the swarm's average total motion after reaching each successive configuration in the desired trajectory. One may note that the swarm's true configuration was measured using an external measurement device. As expected, motion errors increase as the swarm travels away from its original configuration in open-loop control. However, as claimed in this paper, the proposed inchworm motion strategy keeps these errors at very manageable levels.

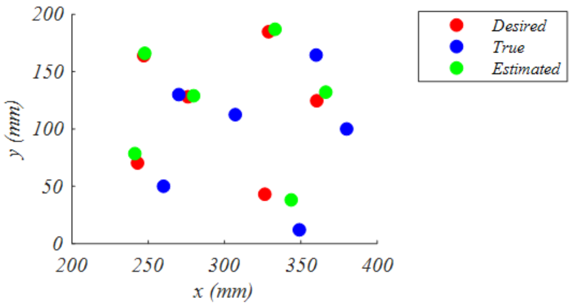

Fig. 16. Experimental results for swarm localization.

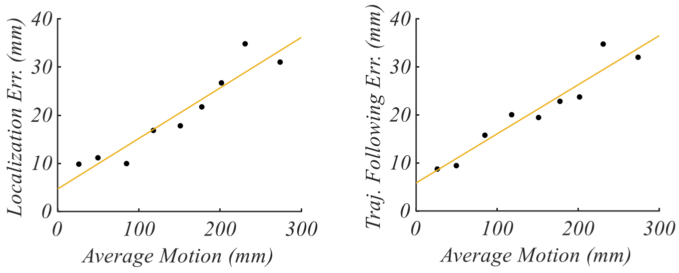

(*a*) (*b*)

Fig. 17. Experimental results: (*a*) localization error, (*b*) trajectory-following error.

7. Comparative Analysis

The proposed inchworm sub-strategy is compared, herein, to an alternate anchor-based method detailed in ref. [57]. The latter divides the swarm into two equal sized subgroups at deployment. The subgroups remain *constant* as the swarm follows a trajectory, namely, their number and choice of member robots do not change.

The comparative analysis was conducted over a series of simulations. In each, a PTP swarm trajectory, comprising $n_d = 100$ desired configurations, was followed. The (cumulative) trajectory-following performance was calculated as trajectory following error at the very last swarm configuration (*i.e.*, when the trajectory was completed):

$$P_f = \frac{\frac{1}{n}\sum_{i=1}^{n_r}\left|{}^{G}\boldsymbol{x}_{tfi}-{}^{G}\boldsymbol{x}_{dfi}\right|}{\bar{m}}, \tag{24}$$

where ${}^{G}\boldsymbol{x}_{tfi}$ and ${}^{G}\boldsymbol{x}_{dfi}$ are, respectively, the ***final true*** and ***desired*** positions of Robot *i* at C_{dn_d}. The trajectory-following performance metric is normalized with respect to the average total motion of all robots, $\bar{m}$:

$$\bar{m} = \sum_{j=1}^{n_d}\left(\frac{1}{n}\sum_{i=1}^{n_r}\left|{}^{G}\boldsymbol{x}_{tn_{sj}i} - {}^{G}\boldsymbol{x}_{tn_{s(j-1)}i}\right|\right) \tag{25}$$

where ${}^{G}\boldsymbol{x}_{tn_{sj}i}$ is the ***true*** position of Robot *i* once all intermediate steps to C_{dj} have been completed.

The results of the simulations are detailed in Table I below. In these simulations, the desired swarm trajectories for a swarm of $n_r = 10$ robots were generated randomly, changing pose and topology at each successive desired configuration. In the inchworm experiments, the optimal anchors were selected through the proposed strategy detailed in Section 4, with $w_v = 0.5$, and $w_l = 0.5$. The anchor robots for the method detailed in ref. [57], however, were selected randomly. Namely, the swarm was randomly divided into two equal sized subgroups at deployment (*i.e.*, $n_a = 5$). All simulations were subjected to random noise in motion command execution and sensing data, as detailed in Section 6 above.

Table I. Comparative Analysis – Results.

	Trajectory Following Performance, P_f	
Strategy	*Sample-Mean*	*Sample-Std-dev*
Ref. [57]	0.0673	0.0500
Our Method	0.0477	0.0354

Comparison of the results illustrates that the proposed inchworm sub-strategy is indeed superior to the method detailed in ref. [57], with a confidence level of at least 97%, Table II below. Both strategies traversed all desired trajectories with an average of $n_a = 5$ anchors, illustrating that, through dynamic anchor selection, the proposed inchworm sub-strategy achieves superior trajectory following performance without suffering from reduced speed.

Table II. Comparative Analysis – Confidence Interval.

Strategy	*Population-Mean, μ, 97% Confidence Interval*
Ref. [57]	[**0.0564 -** 0.0782]
Our Method	[0.0400 - **0.0564**]

8. Conclusions

This paper presents an inchworm-inspired motion planning strategy developed for achieving accurate swarm trajectory following. The proposed strategy divides the swarm into two subgroups of anchor and mobile robots that take turns for incrementally moving towards their destination. Through inter-robot sensing, the two subgroups cooperate and compensate for their motion uncertainty, thus, allowing the swarm to achieve enhanced localization and trajectory following performance.

The proposed inchworm strategy is novel as it dynamically selects the optimal number and choice of anchor robots as the swarm travels through a series of desired configurations. This flexibility feature is used to maximize the swarm's overall motion performance, which consists of two competing objectives – swarm localization and speed. As a result, the proposed strategy achieves superior trajectory following performance, when compared to existing methods. Through dynamic anchor selection, the proposed strategy could also consider other run-time practical constraints, such as the finite sensing range between swarm robots. In doing so, the motion planning and localization problems at hand are decoupled. This allows the proposed inchworm motion strategy to work with any localization method considered.

A complementary swarm localization method, which fuses inter-robot proximity measurements and robot motion commands is also presented. This method is novel as it does not require direct communication between anchor and mobile robots. The proposed localization method is also applicable to non-anchor based swarm motion strategies, as long as the swarm is equipped with the necessary sensing technology.

The inchworm motion strategy was evaluated through a series of physical and simulated experiments. The physical experiments, conducted with a swarm of *mROBerTO* millirobots, illustrated the feasibility of the developed motion planning and localization strategies for real-world applications, such as human swarm interactions. The performance of the developed inchworm strategy was also compared to competing methods through extensive trajectory following simulations. The results illustrate that the proposed strategy achieves significantly superior trajectory following performance, without suffering from reduced swarm speed.

Acknowledgements

The authors would like to acknowledge the support received, in part, by the Natural Sciences and Engineering Research Council of Canada (NSERC).

Competing Interests Declaration

Competing interests: The authors declare none.

References

1. E. Şahin, "Swarm Robotics: From Sources of Inspiration to Domains of Application," **In**: *Swarm Robotics* (2005) pp. 10–20.

2. M. Brambilla, E. Ferrante, M. Birattari, and M. Dorigo, "Swarm robotics: a review from the swarm engineering perspective," *Swarm Intel.* **7**(1), 1–41 (2013).

3. N. Nedjah and L. S. Junior, "Review of methodologies and tasks in swarm robotics towards standardization," *Swarm Evol. Comp.* 50, 100565 (2019).

4. M. S. Innocente and P. Grasso, "Self-organising swarms of firefighting drones: Harnessing the power of collective intelligence in decentralised multi-robot systems," J. *Comp. Sci.* 34, 80–101 (2019).

5. P. P. Neumann et al., “Indoor Air Quality Monitoring Using Flying Nanobots: Design and Experimental Study,” **In**: *IEEE International Symposium on Olfaction and Electronic Nose* (2019) pp. 1-3.

6. G. A. Cardona and J. M. Calderon, “Robot swarm navigation and victim detection using rendezvous consensus in search and rescue operations,” *Applied Sciences* **9**(8), (2019).

7. C. Eschke, M. K. Heinrich, M. Wahby, and H. Haman, “Self-Organized Adaptive Paths in Multi-Robot Manufacturing: Reconfigurable and Pattern-Independent Fibre Deployment,” **In**: *IEEE/RSJ International Conference on Intelligent Robots and Systems* (2019) pp. 4086–4091.

8. M. Schranz, M. Umlauft, M. Sende, and W. Elmenreich, “Swarm robotic behaviors and current applications,” *Front. Robot. AI*. **7**, (2020).

9. Z. Kira and M. A. Potter, “Exerting Human Control Over Decentralized Robot Swarms,” **In:** *4th International Conference on Autonomous Robots and Agents* (2009) pp. 566–571.

10. P. Walker, S. A. Amraii, M. Lewis, N. Chakraborty, and K. Sycara, “Human Control of Leader-Based Swarms,” **In**: *IEEE International Conference on Systems, Man, and Cybernetics* (2013) pp. 2712–2717.

11. S. Shahrokhi, L. Lin, C. Ertel, M. Wan, and A. T. Becker, “Steering a swarm of particles using global inputs and swarm statistics,” *IEEE Trans. Robot.* **34**(1), 207–219 (2018).

12. J. Y. Kim, Z. Kashino, T. Colaco, G. Nejat, and B. Benhabib, “Design and implementation of a millirobot for swarm studies – mROBerTO,” *Robotica* **36**(11), 1591–1612 (2018).

13. J. Y. Kim, T. Colaco, Z. Kashino, G. Nejat, and B. Benhabib, “mROBerTO: A Modular Millirobot for Swarm-Behavior Studies,” **In**: *IEEE/RSJ International Conference on Intelligent Robots and Systems* (2016) pp. 2109–2114.

14. K. Eshaghi, Y. Li, Z. Kashino, G. Nejat, and B. Benhabib, “mROBerTO 2.0 – An autonomous millirobot with enhanced locomotion for swarm robotics,” *Robotic. Automat. Let.* **5**(2), 962–969 (2020).

15. W. Ren and R. Beard, “A decentralized scheme for spacecraft formation flying via the virtual structure approach,” *J. Guide., Control, Dyn*. **27**, 1746–1751 (2004).

16. I. Vatamaniuk, G. Panina, A. Saveliev, and A. Ronzhin, “Convex Shape Generation by Robotic Swarm,” **In**: *International Conference on Autonomous Robot Systems and Competitions* (2016) pp. 300–304.

17. M. P. Vicmudo, E. P. Dadios, and R. R. P. Vicerra, “Path Planning of Underwater Swarm Robots Using Genetic Algorithm,” **In**: *International Conference on Humanoid, Nanotechnology, Information Technology, Communication and Control, Environment and Management* (2014) pp. 1-5.

18. H.-X. Wei, Q. Mao, Y. Guan, and Y.-D. Li, “A centroidal Voronoi tessellation based intelligent control algorithm for the self-assembly path planning of swarm robots,” *Exp. Syst. App.* **85**, 261–269 (2017).

19. Y.-T. Lee, S.-F. Zeng, and C.-S. Chiu, “Distributed Path Planning of Swarm Mobile Robots,” **In**: *12th Asian Control Conference* (2019) pp. 49–54.

20. W. Hönig, J. A. Preiss, T. K. S. Kumar, G. S. Sukhatme, and N. Ayanian, “Trajectory planning for quadrotor swarms,” *IEEE Trans. Robot.* **34**(4), 856–869 (2018).

21. D. Izzo and Pettazzi, “Equilibrium Shaping: Distributed Motion Planning for Satellite Swarm,” **In**: *8th International Symposium on Artificial Intelligence, Robotics and Automation in Space* (2005).

22. V. Gazi, “Swarm aggregations using artificial potentials and sliding-mode control,” *IEEE Trans. Robot.* **21**(6), 1208–1214 (2005).

23. J. R. T. Lawton, R. W. Beard, and B. J. Young, “A decentralized approach to formation maneuvers,” *IEEE Trans. Robot. Autom.* **19**(6), 933–941 (2003).

24. D. Xu, X. Zhang, Z. Zhu, C. Chen, and P. Yang, “Behavior-based formation control of swarm robots,” *Mathem. Prob. Eng.* (2014).

25. C. Bentes and O. Saotome, “Dynamic Swarm Formation with Potential Fields and A* Path Planning in 3D Environment,” **In**: *Brazilian Robotics Symposium and Latin American Robotics Symposium* (2012) pp. 74–78.

26. T. Soleymani and F. Saghafi, “Behavior-Based Acceleration Commanded Formation Flight Control,” **In**: *International Conference on Control, Automation and Systems* (2010) pp. 1340–1345.

27. L. Consolini, F. Morbidi, D. Prattichizzo, and M. Tosques, “A Geometric Characterization of Leader-Follower Formation Control,” **In**: *IEEE International Conference on Robotics and Automation* (2007) pp. 2397–2402.

28. H. Wang, D. Guo, X. Liang, W. Chen, G. Hu, and K. K. Leang, “Adaptive vision-based leader–follower formation control of mobile robots,” *Trans. Indust. Electron.* **64**(4), 2893–2902 (2017).

29. C.-C. Lin, K.-C. Chen, and W.-J. Chuang, “Motion planning using a memetic evolution algorithm for swarm robots,” *Int. J. Adv. Rob. Syst.* **9**(1), 19 (2012).

30. K. D. Do and J. Pan, “Nonlinear formation control of unicycle-type mobile robots,” *Rob. Auton. Syst.* **55**(3), 191–204 (2007).

31. S. M. Ahmadi, H. Kebriaei, and H. Moradi, “Constrained coverage path planning: evolutionary and classical approaches,” *Robotica* **36**(6), 904–924 (2018).

32. Y. Chen, S. Ren, Z. Chen, M. Chen, and H. Wu, “Path planning for vehicle-borne system consisting of multi air–ground robots,” *Robotica* **38**(3), 493–511 (2020).

33. A. Ashraf, A. Majd, and E. Troubitsyna, “Online path generation and navigation for swarms of UAVs,” *Sci. Program.* **2020,** e8530763 (2020).

34. A. Cornejo and R. Nagpal, “Distributed Range-Based Relative Localization of Robot Swarms,” **In**: *Selected Contributions of the Eleventh International Workshop on the Algorithmic Foundations of Robotics.* (2015) pp.107.

35. S. Zhang, E. Staudinger, S. Sand, R. Raulefs, and A. Dammann, “Anchor-Free Localization Using Round-Trip Delay Measurements for Martian Swarm Exploration,” **In**: *IEEE/ION Position, Location and Navigation Symposium* (2014) pp. 1130–1139.

36. M. Berger, L. M. Seversky, and D. S. Brown, “Classifying Swarm Behavior via Compressive Subspace Learning,” **In**: *IEEE International Conference on Robotics and Automation* (2016) pp. 5328–5335.

37. G. Wagner and H. Choset, “Gaussian Reconstruction of Swarm Behavior from Partial Data,” **In**: *IEEE International Conference on Robotics and Automation* (2015) pp. 5864–5870.

38. D. S. Brown and M. A. Goodrich, “Limited Bandwidth Recognition of Collective Behaviors in Bio-inspired swarms,” **In**: *13th International Conference on Autonomous Agents and Multiagent Systems* (2015) pp. 405–412.

39. R. A. Freeman, Peng Yang, and K. M. Lynch, “Distributed Estimation and Control of Swarm Formation Statistics,” **In**: *American Control Conference* (2006) pp. 7.

40. J. Klingner, N. Ahmed, and N. Correll, “Fault-Tolerant Covariance Intersection for Localizing Robot Swarms,” **In**: *Distributed Autonomous Robotic Systems* (2019) pp. 485-497.

41. S. Mayya, P. Pierpaoli, G. Nair, and M. Egerstedt, “Localization in densely packed swarms using interrobot collisions as a sensing modality,” *IEEE Trans. Robotic*. **35**(1), 21–34 (2019).

42. D. Ma, M. J. Er, B. Wang, and H. B. Lim, “Range-free wireless sensor networks localization based on hop-count quantization,” *Telecomm. Syst*. **50**(3), 199–213 (2012).

43. S. Fukui and K. Naruse, “Swarm EKF Localization for a Multiple Robot System with Range-Only Measurements,” **In**: *IEEE/SICE International Symposium on System Integration* (2013) pp. 796–801.

44. D. Inoue, D. Murai, Y. Ikuta, and H. Yoshida, “Distributed Range-Based Localization for Swarm Robot Systems using Sensor-Fusion Technique,” **In**: *8th International Conference on Sensor Networks* (2019) pp. 13–22.

45. J. Y. Kim et al., “A high-performance millirobot for swarm-behaviour studies: Swarm-topology estimation,” *Int. J. Adv. Rob. Syst*. **16**(6), (2019).

46. W. Bezouska and D. Barnhart, “Decentralized Cooperative Localization with Relative Pose Estimation for a Spacecraft Swarm,” **In**: *IEEE Aerospace Conference* (2019) pp. 1–13.

47. A. G. Pires, D. G. Macharet, and L. Chaimowicz, “Exploring Heterogeneity for Cooperative Localization in Swarm Robotics,” **In**: *International Conference on Advanced Robotics* (2015) pp. 407–414.

48. H. Wu, S. Qu, D. Xu, and C. Chen, “Precise localization and formation control of swarm robots via wireless sensor networks,” *Mathem. Prob. Eng.* **2014,** 1–12 (2014).

49. J. Gutmann, P. Fong, and M. E. Munich, “Localization in a Vector Field Map,” **In**: *International Conference on Intelligent Robots and Systems* (2012) pp. 3144–3151.

50. E. Olson, “AprilTag: A Robust and Flexible Visual Fiducial System,” **In**: *International Conference on Robotics and Automation* (2011) pp. 3400–3407.

51. T. Krajník, M. Nitsche, J. Faigl, T. Duckett, M. Mejail, and L. Přeučil, “External Localization System for Mobile Robotics,” **In**: *International Conference on Advanced Robotics* (2013) pp. 1–6.

52. “Motion Capture Systems,” *OptiTrack*. http://optitrack.com (accessed Jan. 07, 2021).

53. L. E. Navarro-Serment, C. J. J. Paredis, and P. K. Khosla, “A Beacon System for the Localization of Distributed Robotic Teams,” **In**: *International Conference on Field Service Robotics* (1999) pp. 232–237.

54. R. Kurazume, S. Nagata, and S. Hirose, “Cooperative Positioning with Multiple Robots,” **In**: *IEEE International Conference on Robotics and Automation* (1994) pp. 1250–1257.

55. S. Tully, G. Kantor, and H. Choset, “Leap-Frog Path Design for Multi-Robot Cooperative Localization,” **In**: *Field and Service Robotics* (2010) pp. 307–317.

56. S. Xu, Z. Ji, D. T. Pham, and F. Yu, “Simultaneous localization and mapping: swarm robot mutual localization and sonar arc bidirectional carving mapping,” *Proceed. Instit. Mech. Eng. Part C: J. Mech. Eng. Sc.* **225**(3) 733–744 (2011).

57. A. G. Pires, D. G. Macharet, and L. Chaimowicz, “Towards Cooperative Localization in Robotic Swarms,” **In**: *Distributed Autonomous Robotic Systems* (2016) pp. 105–118.

58. S. Thrun, W. Burgard, D. Fox, and R. C. Arkin, “The GraphSLAM Algorithm,” *Probabilistic Robotics* (2005) MIT Press.

Appendix A: Heuristic for optimal anchor selection

An extensive series of simulations were conducted to evaluate the performance of the proposed heuristic for optimal anchor selection, detailed in Section 4.2.2. One may recall that the heuristic proposes to select anchor robots which maximize distribution and minimize separation for each step of the inchworm motion strategy.

In the simulations detailed below, a swarm of n robots was instructed to move from one starting configuration to a random desired configuration, using the inchworm motion sub-strategy. In each incremental step, a fixed number of n_a robots were designated as stationary anchors, while the remaining robots moved towards their destination. Furthermore, for each step, the anchor robots were selected using the proposed heuristic. Once the inchworm motion was completed, noisy inter-robot sensor measurements were simulated and used to estimate the swarm’s post motion configuration. The results of the simulated motion and subsequent estimations were evaluated terms of the localization error, $e_l(n_a, \boldsymbol{R}_a)$, Eq. (8), and compared to the performance of a swarm where anchors were selected randomly.

1,000 random experiments were simulated for a swarm size of $n_r = 10$ robots, where $n_a = 5$ robots remain stationary at a time. All simulations were initialized with the same uncertain estimate of the swarm’s initial configuration, C_c. The simulations, however, were subjected to different levels of noise in their inter-robot sensing and motion command executions.

Fig. A1(*a*)-(*b*) below shows the results obtained for (*a*) anchors found through the proposed heuristic, (*b*) randomly chosen anchors, respectively. The anchors determined through the proposed heuristic, Fig. A1(*a*), certainly outperform the random choice of anchors that can be used as initial guesses, Fig. A1(*b*).

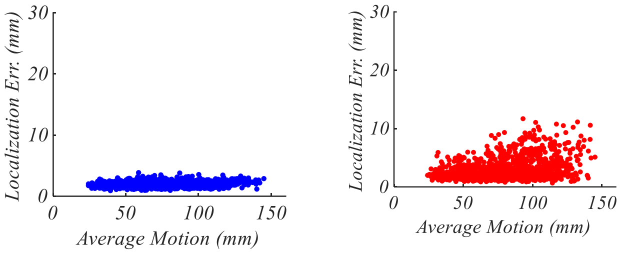

(*a*) (*b*)

Fig. A1. Swarm localization errors for different combinations of anchors: (*a*) anchors found with proposed heuristic, (*b*) random anchors.

Appendix B: Swarm topology estimation

Herein, we consider an alternate formulation to the swarm-topology estimation problem, developed in response to the computational demands of our previous approach.[38]

Let us consider the inter-robot sensor measurements, ρ_{ij} and φ_{ij}, detailed in Section 5, representing the relative position of Robot *j* with respect to Robot *i*, as observed from the reference frame of Robot *i*, in polar coordinates, Fig. B1 below.

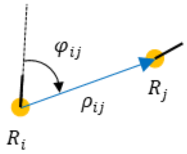

Fig. B1: Inter-robot sensor measurements, thick black lines represent robot orientations.

Such local inter-robot measurements can be transformed to Cartesian coordinates through a simple transformation:

$$\boldsymbol{z}_{ij} = \left(x_{ij},\, y_{ij} \right), \tag{B1}$$

where $x_{ij} = \rho_{ij}\cos\left(\varphi_{ij}\right)$, and $y_{ij} = \rho_{ij}\sin\left(\varphi_{ij}\right)$, respectively.

The estimate of the topology of the swarm (*i.e.*, the position of all robots with respect to a local frame) can, then, be solved for via the following minimization formulation:

$$\left\{{}^{L}\boldsymbol{x}_i^*\right\}_{i=1}^{n_r} = \underset{\left\{{}^{L}\boldsymbol{x}_i\right\}_{i=1}^{n_r}}{\arg\min}\, Q \tag{$B2$}$$

where:

$$Q = \sum_{i=1}^{n_r}\sum_{j=1}^{n_r, j\neq i}\frac{\lambda_{ij}}{2}\left|{}^{L}\boldsymbol{x}_{ij} - {}^{L}\overline{\boldsymbol{x}}_j\right|^2, \text{ and} \tag{B3}$$

$${}^{L}\boldsymbol{x}_{ij} = \begin{bmatrix} x_{ij}\cos\left({}^{L}\theta_i\right) - y_{ij}\sin\left({}^{L}\theta_i\right) + {}^{L}x_i \\ x_{ij}\sin\left({}^{L}\theta_i\right) + y_{ij}\cos\left({}^{L}\theta_i\right) + {}^{L}y_i \end{bmatrix}. \tag{B4}$$

Above, ${}^{L}\bar{\boldsymbol{x}}_j$ is the average position of Robot j and ${}^{L}\theta_i$ is the estimated orientation of Robot i, as observed from the swarm's local reference frame. λ_{ij} is the observance indicator of Robot j by Robot i:

$$\lambda_{ij} = \begin{cases} 1 & \text{if robot } j \text{ is observed by } i \\ 0 & \text{otherwise} \end{cases}. \tag{B5}$$

The solution to minimizing the proposed objective function is the estimated topology of the swarm and the orientation of all robots, with respect to the local frame. However, the inter-robot sensing data available from each robot also provides additional estimates of the positions of neighboring robots. This is illustrated in Fig. B2 below, where the estimated topology of the swarm, determined by solving Eq. (B2) is shown in gray, while the estimated robot positions based on inter-robot sensing measurements are shown in blue. Here, [*i*,*j*] represents the position of Robot *j*, as observed by Robot *i* (i.e., [1,2] is the position of Robot 2, as observed by Robot 1). The estimated swarm topology, $\{{}^{L}\hat{\boldsymbol{x}}_i\}_{i=1}^{n_r}$, shown in yellow, is, then, calculated as the centroid position of all available observations. Moreover, the uncertainty in the estimated position of each robot is calculated as the standard deviation in the cluster of points representing the position of each robot:

$$\delta_{pi} = \left|\sigma_{xi}^2 + \sigma_{yi}^2\right|, \tag{B6}$$

where σ_{xi} and σ_{yi} are the standard deviations of the cluster of points associated with Robot *i*.

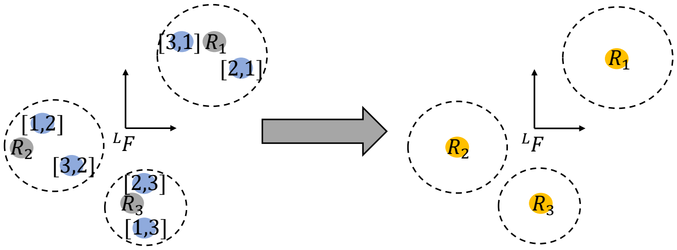

Fig. B2: Swarm-topology estimation.